

PAPER • OPEN ACCESS

Development of $\text{Sr}_{0.6}\text{Ba}_{0.4}\text{Ce}_{0.9}\text{Pr}_{0.1}\text{O}_{3-\delta}$ Electrolyte for Proton-Conducting Solid Oxide Fuel Cell Application

To cite this article: N W Norman *et al* 2019 *IOP Conf. Ser.: Earth Environ. Sci.* **268** 012147

View the [article online](#) for updates and enhancements.

Development of $\text{Sr}_{0.6}\text{Ba}_{0.4}\text{Ce}_{0.9}\text{Pr}_{0.1}\text{O}_{3-\delta}$ Electrolyte for Proton-Conducting Solid Oxide Fuel Cell Application

N W Norman¹, W N A Wan Yusoff¹, A A Jais¹, M R Somalu^{1,*} and A Muchtar^{1,2}

¹Fuel Cell Institute, Universiti Kebangsaan Malaysia, 43600 UKM Bangi, Selangor, Malaysia

²Centre for Materials Engineering and Smart Manufacturing (MERCU), Faculty of Engineering and Built Environment, Universiti Kebangsaan Malaysia, 43600 UKM Bangi, Selangor, Malaysia

*Corresponding author e-mail: mahen@ukm.edu.my

Abstract. $\text{Sr}_{0.6}\text{Ba}_{0.4}\text{Ce}_{0.9}\text{Pr}_{0.1}\text{O}_{3-\delta}$ is synthesized by the glycine–nitrate method. The synthesized powder and resultant electrolyte pellet are systematically characterised for proton-conducting solid oxide fuel cell application. The thermal decomposition and purity of the electrolyte powder were analysed by thermogravimetric analysis (TGA) and X-ray diffraction (XRD), respectively. The morphological structure and chemical stability of the electrolyte pellets are examined by field-emission scanning electron microscopy (FESEM) and XRD, respectively. The selective material decomposes at 1000 °C as recorded by TGA. The calcined powder at 1000 °C is used to produce the electrolyte pellet. The pellet sintered at 1400 °C achieves the average relative density of 94% as measured by Archimedes' method and displays good grain growth with a visible grain boundary. The chemical stability of the pellet is also determined under boiling water for 2 h. The tolerance towards H_2O for the sample improved with the presence of Sr upon exposure to boiling water even though some amorphous phase forms. Based on the result, $\text{Sr}_{0.6}\text{Ba}_{0.4}\text{Ce}_{0.9}\text{Pr}_{0.1}\text{O}_{3-\delta}$ is considered as a potential electrolyte for proton-conducting solid oxide fuel cells.

1. Introduction

Proton-conducting solid oxide fuel cells (H-SOFCs) have been introduced to substitute for conventional oxide-ion-conducting solid oxide fuel cells because of H-SOFCs' ability to operate at low temperatures (500–700 °C). Proton conductors can operate at low temperatures because of the low activation energy required for conduction [1,2]. The development of H-SOFCs electrolyte has been emphasized in producing high proton-conductive with a stable structure and the ability to attain good chemical stability at intermediate temperature by the fellow researchers [3].

Perovskite-type oxide materials (ABO_3) such as SrCeO_3 , BaCeO_3 and BaZrO_3 have been widely studied because of the improved properties that they exhibit (e.g., high proton conductivity) when properly substituted with rare-earth oxides on the A- or B-site [4]. BaCeO_3 has high conductivity, but its instability in air containing CO_2 limits its practical applications. Differently, BaZrO_3 has better chemical stability, but its high sintering temperature causes a highly resistive grain boundary. As a result, this led to low total conductivity that hindered its applications [5]. Although SrCeO_3 exhibited considerable proton conduction, some materials have often been rejected for use in commercial devices because of their unsatisfactory mechanical properties and chemical stability [6]. However, their stability can be reportedly improved without the introduction of Zr into B-sites by using elements such as indium, gallium and praseodymium, thereby removing the requirements on high sintering temperature



[7]. Researchers attempted to pair both chemical stability and proton conductivity performance into single-proton conduction by doping either of two types of materials or by optimizing the composition of their solid solution [8]. The introduction of doping ions at the A- or B-site for the ABO_3 structure for the purpose of overcoming the stability issue was reported. For example, doped $BaCeO_3$ and $SrCeO_3$ at the B-site were proven to produce high conductivity and stability. Besides, the A-site doping which influences on conductivity and stability issues was also reported. [9].

The strategy of doping barium at A-site and praseodymium at B-site was established to simultaneously maximize the sinterability and morphology of the electrolyte. Pr was selected as a doping element considering that doped $BaPrO_3$ compounds can be easily sintered at a relatively low temperature (1400 °C) [10]. The introduction of dopants such as praseodymium at the B-site was found to demonstrate a good stability [7]. Magrasó et al. recorded that the change in the amount of Pr in $BaZrO_3$ improved the chemical stability and proton conductivity. Also, the presence of Pr in $BaZrO_3$ reduced the sintering temperature and maintained the good average grain size [11]. In this present work, the effects of introducing Pr as dopant on the structural and morphological characteristics of the electrolyte were investigated using thermogravimetric analysis (TGA), X-ray diffraction (XRD), and field-emission scanning electron microscopy (FESEM). Thus, the objective of this work will include the morphology and chemical stability of the synthesized material which are critical in evaluating the potential SOFC application of the electrolyte.

2. Methodology

$Sr_{0.6}Ba_{0.4}Ce_{0.9}Pr_{0.1}O_{3-\delta}$ electrolyte powder was prepared by the glycine–nitrate process. A stoichiometric amount of $Sr(NO_3)_2$, $Ba(NO_3)_2$, $Ce(NO_3)_3 \cdot 6H_2O$, and $Pr(NO_3)_3 \cdot 6H_2O$ were dissolved in deionized water. Glycine was added onto the solution to serve as a fuel for combustion [12]. The solution was heated at 300 °C until it spontaneously combusted and precursor powders formed.

The as-precursor powders were characterized by TGA and XRD. TGA was conducted from 25 °C to 1400 °C at a 10 °C min⁻¹ heating/cooling rate by using a thermogravimetric instrument (TG, Mettler Toledo, USA). The as-prepared precursor powders subjected to TGA were then calcined at 1000 °C for 5 h in a high-temperature furnace (Berkeley Scientific BSK-1700X-S, USA). XRD analysis was performed to investigate the powder phase structure using (XRD Bruker D8-Advance, Germany) at the angle of diffraction 2θ within the range of 20° to 80° with a value of $\lambda = 0.15406$ Å.

For morphological characterisation, the calcined electrolyte powders were suppressed into pellets and sintered at 1400 °C for 5 h at a heating/cooling rate of 10 °C min⁻¹ in a high-temperature furnace (Berkeley Scientific BSK-1700X-S, USA). The relative density of the pellets was determined through Archimedes' method and analyzed by FESEM (JEOL JSM-6701F, Japan). The chemical stability of $Sr_{0.6}Ba_{0.4}Ce_{0.9}Pr_{0.1}O_{3-\delta}$ was evaluated by exposing the sintered pellets to boiling water for 2 h and then subjecting to XRD analysis.

3. Result and Discussion

3.1 Thermal analysis

The TGA recorded are shown in Figure 1. Based on thermogravimetric and differential thermal analysis, the powder experienced weight loss in two parts at 25 °C to 1400 °C. The first weight loss occurred at $T < 460$ °C, which indicated dehydration and the decomposition of metal nitrates and unreacted glycine (glycine normally decomposes at 240 °C). The major weight loss starting at ~700 °C resulted from the decomposition of carbonaceous residue [13]. After crossing both parts, no further weight loss found thus indicated on the formation of $Sr_{0.6}Ba_{0.4}Ce_{0.9}Pr_{0.1}O_{3-\delta}$ electrolyte. Thermal decomposition analysis indicated that the minimum recommended temperature for the calcination of $Sr_{0.6}Ba_{0.4}Ce_{0.9}Pr_{0.1}O_{3-\delta}$ powder was 1000 °C.

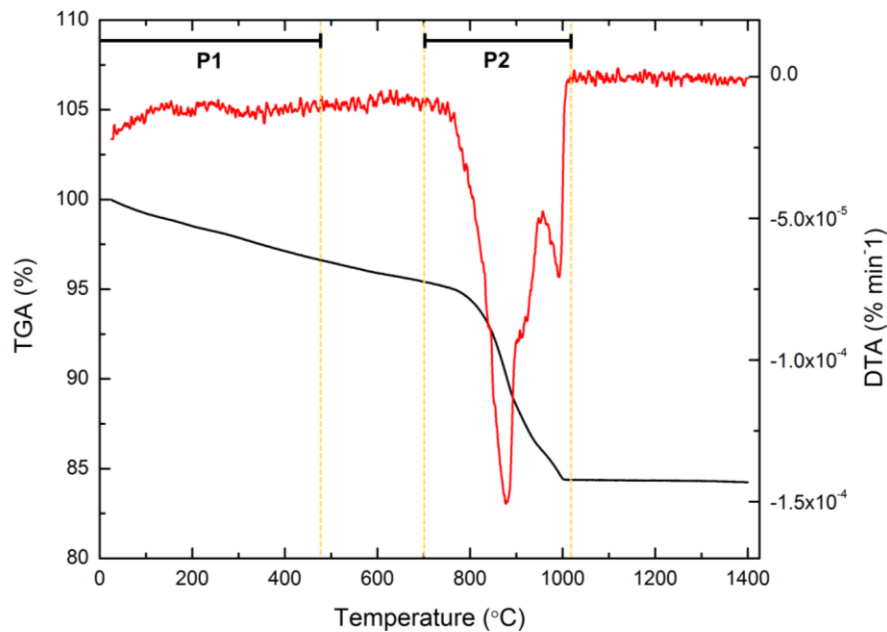


Figure 1. TG/DTA curves of $\text{Sr}_{0.6}\text{Ba}_{0.4}\text{Ce}_{0.9}\text{Pr}_{0.1}\text{O}_{3-\delta}$ powders at 25 °C to 1400 °C

3.2 Crystallographic analysis

Figure 2 shows the XRD patterns of $\text{Sr}_{0.6}\text{Ba}_{0.4}\text{Ce}_{0.9}\text{Pr}_{0.1}\text{O}_{3-\delta}$ powders obtained at 1000 °C calcination temperature for 5 h. $\text{Sr}_{0.6}\text{Ba}_{0.4}\text{Ce}_{0.9}\text{Pr}_{0.1}\text{O}_{3-\delta}$ already crystallized at this temperature. The presence of Ba and Pr in the XRD profile indicated that they were already doped into the material. However, the formation of traces of CeO_2 -like phase can be found at 1000 °C, and this formation may have occurred because the Sr content was insufficient to suppress the formation of CeO_2 -like phase [3].

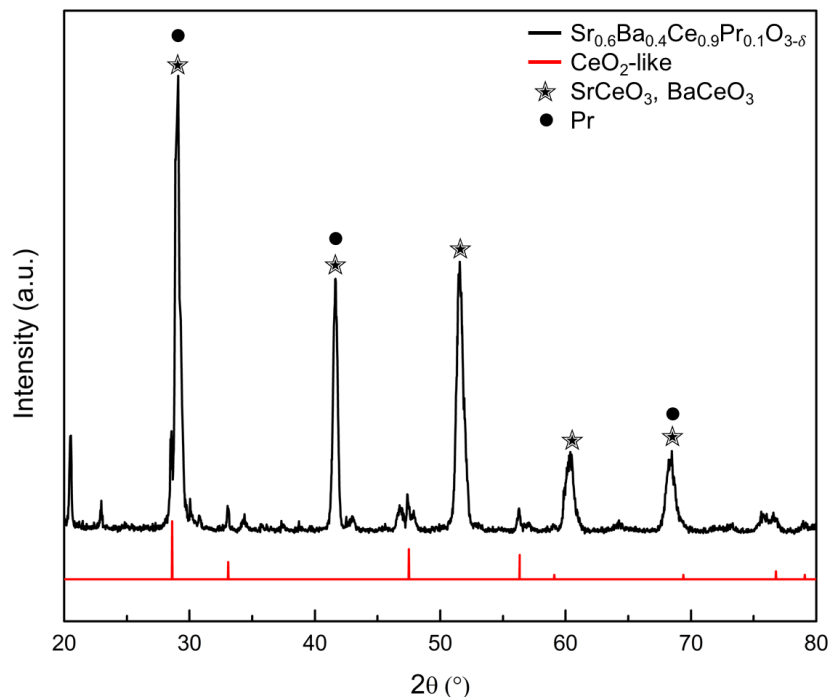


Figure 2. XRD patterns of $\text{Sr}_{0.6}\text{Ba}_{0.4}\text{Ce}_{0.9}\text{Pr}_{0.1}\text{O}_{3-\delta}$ powders calcined at 1000 °C

3.3 Morphological analysis

The cross-section and surface microstructure of the $\text{Sr}_{0.6}\text{Ba}_{0.4}\text{Ce}_{0.9}\text{Pr}_{0.1}\text{O}_{3-\delta}$ pellet obtained by FESEM analysis is shown in Figure 3. The sintered pellet of 1400 °C was compact, fully dense, and well distributed with non-uniform grains. The average particle in the region size was approximately 15 μm . However, slight porosity was observed at the cross-section of the electrolyte. The average specific density obtained from this electrolyte was 94%, which was deemed fit for its application as a proton-conducting electrolyte as shown in Table 1. Consequently, it is clear that the addition of Pr promotes both sintering and grain growth, and thereby that praseodymium can be considered a sintering aid as suggested previously [10]. Larger grain sizes of electrolyte material can offer weaker overall grain boundary resistance, whereas denser grains favor ion migration and electron blocking [14,15].

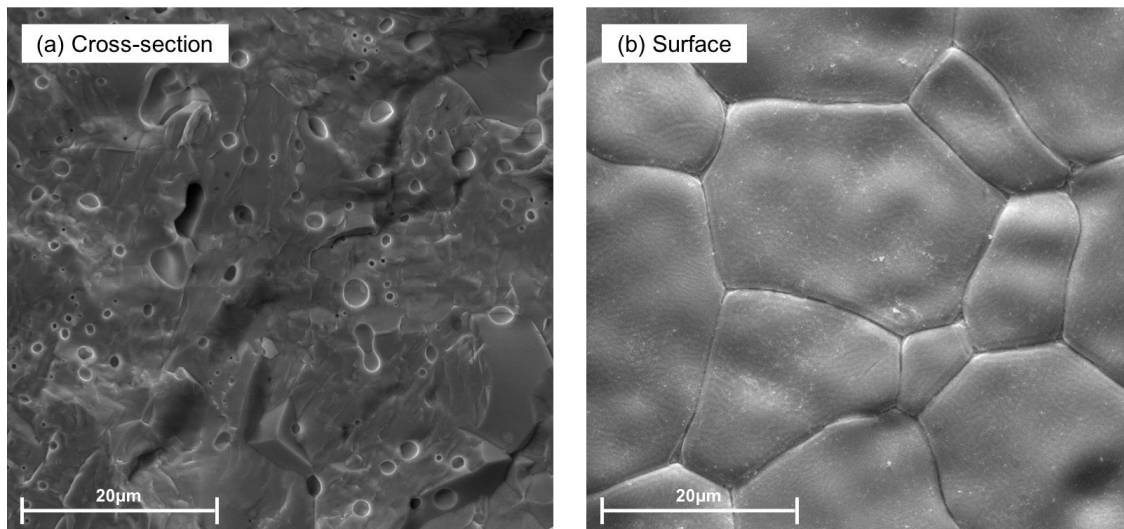


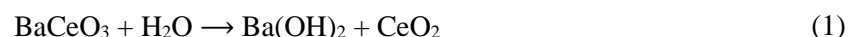
Figure 3. Morphologies of $\text{Sr}_{0.6}\text{Ba}_{0.4}\text{Ce}_{0.9}\text{Pr}_{0.1}\text{O}_{3-\delta}$ electrolyte after sintering at 1400 °C

Table 1. The relative density of doped Pr electrolyte pellet

Samples	Sintering temperature (C)	Time (h)	Relative density (%)	Ref
$\text{Sr}_{0.6}\text{Ba}_{0.4}\text{Ce}_{0.9}\text{Pr}_{0.1}\text{O}_{3-\delta}$	1400	5	94	This work
$\text{BaCe}_{0.7}\text{Y}_{0.2}\text{Pr}_{0.1}\text{O}_{3-\delta}$	1500	1	98	[7]
$\text{BaZr}_{0.7}\text{Pr}_{0.1}\text{Y}_{0.2}\text{O}_{3-\delta}$	1500	8	94	[10]
$\text{BaZr}_{0.3}\text{Pr}_{0.6}\text{Gd}_{0.1}\text{O}_{3-\delta}$	1500	5	92	[11]

3.4 Chemical stability in H_2O atmosphere

Since the end product of electrochemical process in H-SOFCs application is water, the electrolyte constantly meets this atmosphere at high temperature. Thus, the $\text{Sr}_{0.6}\text{Ba}_{0.4}\text{Ce}_{0.9}\text{Pr}_{0.1}\text{O}_{3-\delta}$ pellet was studied in a moist atmosphere of boiling water for 2 h to evaluate their stability. The XRD pattern of $\text{Sr}_{0.6}\text{Ba}_{0.4}\text{Ce}_{0.9}\text{Pr}_{0.1}\text{O}_{3-\delta}$ compositions recorded before and after exposure are shown in Figure 4. BaCeO_3 was unstable in a water-containing atmosphere at high temperatures due to the formation of hydroxides, which can be shown using the decomposition reaction:



Wang et al. evaluated the stability of $\text{Ba}_{1-x}\text{Sr}_x\text{Ce}_{0.8}\text{Y}_{0.2}\text{O}_{3-\delta}$ (BSCY; $x = 0, 0.1, 0.2, 0.5, 1$) in boiling water sintered with different contents of strontium. Their results showed that the XRD pattern changes after exposure, i.e., the impurity peaks of high Sr content become insignificant. These findings indicated that the stability of water was already enhanced [9]. Mahadik et al. also found that the existence of strontium at A-site take on an important role in the stability enhancement against H_2O than barium-based compositions [16].

The crystallinity percentage after exposure (64.4%) decreased compared with the one before exposure (86.9%). Yellowish powder found after the exposure which indicated the presence of CeO_2 while a part of the pellet started to disperse into the water after 2 hours. The presence of CeO_2 , Ba(OH)_2 , and BaCO_3 were found through XRD after exposure as shown in the reaction. The peaks of Sr were found to be stable, indicating that the Sr content enhanced the stability of the materials in water. However, the formation of BaCeO_3 may have been distributed during the exposure, i.e., wherein BaCeO_3 may reacted with CO_2 in water or from the air [9].

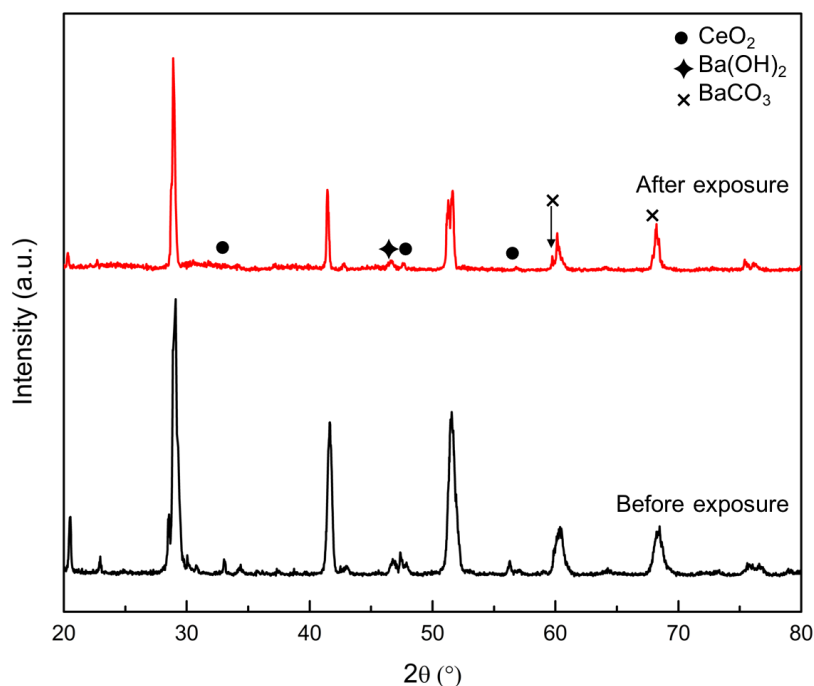


Figure 4. XRD patterns of sintered $\text{Sr}_{0.6}\text{Ba}_{0.4}\text{Ce}_{0.9}\text{Pr}_{0.1}\text{O}_{3-\delta}$ before and after exposure to H_2O at $100\text{ }^\circ\text{C}$ for 2 h

4. Conclusion

$\text{Sr}_{0.6}\text{Ba}_{0.4}\text{Ce}_{0.9}\text{Pr}_{0.1}\text{O}_{3-\delta}$ electrolyte powder has been successfully prepared using the glycine–nitrate process. Analysis of thermal composition revealed that the powder decomposed and contained water, glycine, metal nitrates, and carbonaceous residue. The temperature of $1000\text{ }^\circ\text{C}$ was found to be the minimum required temperature for calcination. The pellet sintered at $1400\text{ }^\circ\text{C}$ also exhibited compact and well-distributed grains with improved density of around 94%. The pellet was also found to show some new formation after exposure in boiling water. However, further analyses should be done onto the performance of $\text{Sr}_{0.6}\text{Ba}_{0.4}\text{Ce}_{0.9}\text{Pr}_{0.1}\text{O}_{3-\delta}$ electrolyte. Further improvement can be made by increasing the mixing time from 12 h to 24 h to enhance the purity of $\text{Sr}_{0.6}\text{Ba}_{0.4}\text{Ce}_{0.9}\text{Pr}_{0.1}\text{O}_{3-\delta}$ electrolyte powder.

Acknowledgment

The authors thank the Ministry of Higher Education and Universiti Kebangsaan Malaysia for their funding support through the research sponsorship of DIP-2018-040. The Centre for Research and Instrumentation Management, UKM, Fuel Cell Institute, UKM, Institute of Advanced Technology, UPM, and Imaging Centre, Faculty of Pharmacy, UiTM Puncak Alam are also acknowledged for letting us use their excellent preparation and testing facilities.

References

- [1] Hossain S, Abdalla AM, Zaini JH, Savaniu CD, Irvine JTS and Azad AK 2017 Highly dense and novel proton conducting materials for SOFC electrolyte *Int. J. Hydrogen Energy* **42** 27308
- [2] Wan Yusoff WNA, Norman NW, Abdul Samat A, Somalu MR, Muchtar A and Baharuddin NA 2018 Fabrication process of cathode materials for solid oxide fuel cell *J. Adv. Res. Fluid Mech. Therm. Sci.* **50** 153
- [3] Lee KR, Tseng CJ, Chang JK, Hung IM, Lin JC and Lee SW 2013 Strontium doping effect on phase

- homogeneity and conductivity of $\text{Ba}_{1-x}\text{Sr}_x\text{Ce}_{0.6}\text{Zr}_{0.2}\text{Y}_{0.2}\text{O}_{3-\delta}$ proton-conducting oxides *Int. J. Hydrogen Energy* **38** 11097
- [4] Sugimoto T, Hasegawa S and Hashimoto T 2012 Phase transition behavior of mother phase of proton-conducting oxides, $\text{Sr}_{1-x}\text{Ba}_x\text{ZrO}_{3-\delta}$ *Thermochim. Acta* **530** 58
- [5] Zhu Z, Guo E, Wei Z and Wang H 2018 Tailoring $\text{Ba}_3\text{Ca}_{1.18}\text{Nb}_{1.82}\text{O}_{9-\delta}$ with NiO as electrolyte for proton-conducting solid oxide fuel cells *J. Power Sources* **373** 132
- [6] Dahl PI, Haugrud R, Lein HL, Grande T, Norby T and Einarsrud MA 2007 Synthesis, densification and electrical properties of strontium cerate ceramics *J. Eur. Ceram. Soc.* **27** 4461
- [7] Petit CTG and Tao S 2014 Effects of cobalt addition on structural, thermal and electrical properties of praseodymium-yttrium co-doped barium cerates *J. Electroceramics* **32** 344
- [8] Guangya W and Jingli L 2014 Promoting influence of doping indium into $\text{BaCe}_{0.5}\text{Zr}_{0.3}\text{Y}_{0.2}\text{O}_{3-\delta}$ as solid proton conductor *Int. J. Appl. Ceram. Technol.* **12** 1174
- [9] Wang S, Zhao F, Zhang L, Brinkman K and Chen F 2010 Stability and electrical property of $\text{Ba}_{1-x}\text{Sr}_x\text{Ce}_{0.8}\text{Y}_{0.2}\text{O}_{3-\delta}$ high temperature proton conductor *J. Alloys Compd.* **506** 263
- [10] Fabbri E, Bi L, Tanaka H, Pergolesi D and Traversa E 2011 Chemically stable Pr and y Co-doped barium zirconate electrolytes with high proton conductivity for intermediate-temperature solid oxide fuel cells *Adv. Funct. Mater.* **21** 158
- [11] Magrasó A, Frontera C, Gunnæs AE, Tarancón A, Marrero-López D, Norby T and Haugrud R 2011 Structure, chemical stability and mixed proton-electron conductivity in $\text{BaZr}_{0.9-x}\text{Pr}_x\text{Gd}_{0.1}\text{O}_{3-\delta}$ *J. Power Sources* **196** 9141
- [12] Ding X, Ding L, Wang L, Zhu W, Hua G, Liu H, Gao Z and Yuan G 2017 Improved electrochemical activity and stability of $\text{LaNi}_{0.6}\text{Fe}_{0.4}\text{O}_{3-\delta}$ cathodes achieved by an in-situ reaction *Electrochim. Acta* **236** 378
- [13] Jaiz AA, S A MA, Anwar M, Somalu MR, Muchtar A, Wan Isahak WNR, Chou YT, Singh R and Brandon NP 2017 Enhanced ionic conductivity of scandia-ceria-stabilized-zirconia (10Sc1CeSZ) electrolyte synthesized by the microwave-assisted glycine nitrate process *Ceram. Int.* **43** 8119
- [14] Mumtaz S, Ahmad MA, Raza R, Arshad MS, Ahmed B, Ashiq MN and Abbas G 2017 Nano grained Sr and Zr co-doped BaCeO_3 electrolytes for intermediate temperature solid oxide fuel cells *Ceram. Int.* **43** 14354
- [15] Hossain S, Abdalla AM, Radenahmad N, Zakaria AKM, Zaini JH, Rahman SMH, Eriksson SG, Irvine JTS and Azad AK 2018 Highly dense and chemically stable proton conducting electrolyte sintered at 1200 °C *Int. J. Hydrogen Energy* **43** 894
- [16] Mahadik PS, Jain D, Shirsat AN, Manoj N, Varma S, Wani BN and Bharadwaj SR 2016 Synthesis, stability and conductivity of $\text{SrCe}_{0.8-x}\text{Zr}_x\text{Y}_{0.2}\text{O}_{3-\delta}$ as electrolyte for proton conducting SOFC *Electrochim. Acta* **219** 614